Charge Carrier Extraction in Organic Solar Cells Governed by Steady-State Mobilities

Le Corre, Vincent Marc; Doumon, Nutifafa Y.; Rahimichatri, Azadeh; Koster, L. Jan Anton

Published in:
Advanced Energy Materials

DOI:
10.1002/aenm.201701138

Publication date:
2017

Charge Carrier Extraction in Organic Solar Cells Governed by Steady-State Mobilities

Vincent M. Le Corre, Azadeh Rahimi Chatri, Nutifafa Y. Doumon, and L. Jan Anton Koster**

Charge transport in organic photovoltaic (OPV) devices is often characterized by steady-state mobilities. However, the suitability of steady-state mobilities to describe charge transport has recently been called into question, and it has been argued that dispersion plays a significant role. In this paper, the importance of the dispersion of charge carrier motion on the performance of organic photovoltaic devices is investigated. An experiment to measure the charge extraction time under realistic operating conditions is set up. This experiment is applied to different blends and shows that extraction time is directly related to the geometrical average of the steady-state mobilities. This demonstrates that under realistic operating conditions the steady-state mobilities govern the charge extraction of OPV and gives a valuable insight in device performance.

1. Introduction

In the early 1990s, Sariciftci et al. described the first polymer:fullerene bulk heterojunction (BHJ) solar cell.[1] Since then organic photovoltaic (OPV) devices have attracted a lot of attention in the scientific community. The ability of organic semiconductors to be used in large-scale production and their high efficiency upon low light intensity make them promising materials for harvesting solar energy. The state-of-the-art OPV devices now reach efficiencies up to 11 and 13% for single and multijunction cell devices, respectively.[2] However, despite being studied for decades, the underlying physics of OPVs is not yet fully understood and is still subject to debate.

In highly disordered materials, such as organic semiconductors, charge motion is based on thermally activated hopping.[3] This charge transport mechanism is characterized by lower electron and hole mobility values compared to inorganic semiconductors where band-like transport takes place. The transport in OPV is often described by the steady-state mobilities that can be obtained by a steady-state measurement, such as the space-charge limited current (SCLC) technique.[4]

V. M. Le Corre, A. R. Chatri, N. Y. Doumon, Dr. L. J. A. Koster
Zernike Institute for Advanced Materials
University of Groningen
Nijenborgh 4, 9747 AG, Groningen, The Netherlands
E-mail: v.m.le.corre@rug.nl; l.j.a.koster@rug.nl

The ORCID identification number(s) for the author(s) of this article can be found under https://doi.org/10.1002/aenm.201701138.

DOI: 10.1002/aenm.201701138

However, time-of-flight (TOF) experiments and Monte Carlo (MC) simulations have shown that if the degree of both energetic and positional disorder is high enough, the fluctuations of the intersite distances create fast diffusion routes.[5] These routes increase the mobility of carriers located in high energetic states leading to their extraction before they have the time to thermalize, thus creating dispersion in current extraction on a short time scale.[5]

Although the relative importance of the dispersive effect on OPV devices performance is conflicting in the literature,[6] new reports have suggested that it is necessary to consider the influence of the dispersion effect in current extraction and that steady-state mobilities are not relevant to describe the transport in OPV devices.[6b,c] In their study, they set up a MC simulation and an optoelectrical measurement based on a laser light pulse from which they measured the charge carrier mobility on a time scale of 100 fs after the exciton generation.[6b,c] In the first nanoseconds, they observed a charge carrier mobility orders of magnitude higher than the one measured by steady-state measurements. This high mobility is due to the carriers being excited on the upper part of the DOS that are extracted before losing their energy through thermalization.[6b,c] The authors conclude that the steady-state mobilities are not pertinent to make relevant statements on OPV performance and that the thermalization loss plays a key role in the extraction.

On the other hand, van der Kaap and Koster used a MC simulation to show that in an organic diode the thermalization has a limited impact on the performance.[6a] In addition, other reports have also demonstrated that SCLC analysis can be successfully applied to organic solar cells and gives valuable insight into materials transport properties.[4b,7] In fact, many studies have shown that the power conversion efficiency (PCE)[4b] and fill factor (FF)[7] depend on the steady-state mobilities. Furthermore, it has also been shown that drift-diffusion simulations, which assume a near-equilibrium state and use steady-state mobilities as an input, successfully describe the characteristics of organic transistors, light-emitting diodes, and solar cells.[7a,b,8] Transient signals of OPV devices have also been well reproduced by drift-diffusion simulation. For example, Albrecht et al. have been able to fit the time-delayed collection field (TDCF) signal using drift-diffusion simulations. Even though they also see that during the first 50 ns after the charge generation a small effect of mobility relaxation has to be taken into account in order to reproduce the transient signal, it still shows that those simulations are suitable to describe the transient behavior of organic solar cells.[9] These studies raise

the question of what is the influence of the current dispersion in OPV devices and whether steady-state mobilities can be used or not to characterize the transport and extraction in organic semiconductor devices.

In this study, we demonstrate that there is no need to consider the effect of dispersion and that steady-state mobilities are a suitable way to study the transport and extraction in OPV devices under realistic operating conditions: real OPV device configuration, the use of a multiple wavelength illumination light, and an intensity close to 1 sun. To that purpose, we carried out a combination of transient experiments and simulations to study the extraction in OPV devices. Several donor:acceptor blends have been tested, scanning a wide range of polymers backbones, values and ratio of the mobilities and efficiencies. This allows us to give a picture as broad as possible of what happens in OPV devices, and it shows what happens with some of the best materials to date. Furthermore, these results are supported by transient drift-diffusion simulations performed for a wide range of parameters.

2. Results and Discussion

First, a transient experiment was set up to study the extraction of charges. The dynamics of the charge carriers is studied by measuring the decay of the current density over time between two light intensities for different applied voltages. For $t < 0$, the device is in steady-state condition at the higher light intensity, then at time zero the intensity is slightly reduced. One should note that the bias voltage is kept constant during the reduction of the light. This will result in the extraction of the extra carriers Δq thus leading to a decay in current to reach the steady-state conditions at the lower light intensity; see **Figure 1**.

After the reduction of the light intensity, the charge carrier density will decay to match the steady-state conditions at lower light intensity. The excess charge carriers will move by drift and diffusion toward the electrodes to be extracted, leading to a decay in current density. This decay of the extra charge carriers Δq can be represented by the following equation

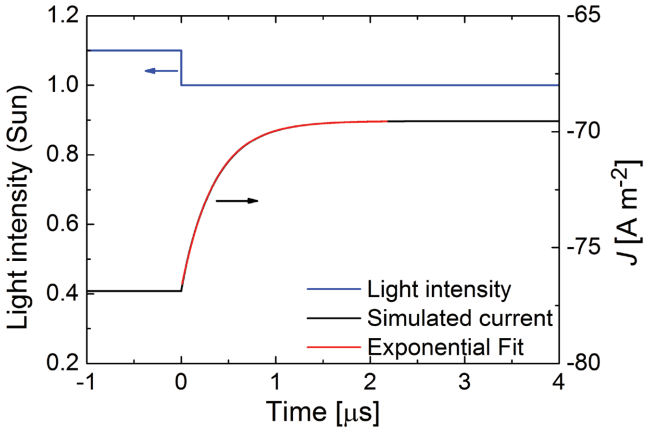

Figure 1. Drift-diffusion simulation results for balanced mobilities, $\mu_n = \mu_p = 1 \times 10^{-7}$ m^2 V^{-1} s^{-1}. The decrease of the generation rate, blue line, which is directly proportional to the reduction of the light intensity, creates a decay of the current.

$$\frac{\partial \Delta q}{\partial t} = -f\,\Delta q \tag{1}$$

where the charge carrier extraction f can be written as the sum of the drift and diffusion rates, f^{Drift} and $f^{\text{Diffusion}}$, respectively, such as[10]

$$f = f^{\text{Drift}} + f^{\text{Diffusion}} \tag{2}$$

Considering that the charge carriers travel on average half of the active layer thickness (L) to be extracted at the electrode and neglecting space-charge effects so that the electrical field can be written as V_{eff}/L with V_{eff} the effective voltage drop across the device, the drift term can be expressed as the inverse of the transit time[10]

$$f^{\text{Drift}} = 2\frac{\mu F}{L} = 2\frac{\mu V_{\text{eff}}}{L^2} \tag{3}$$

where μ is the charge carrier mobility.[10] In the same way, the diffusion contribution can be estimated using the Einstein relation[10]

$$f^{\text{Diffusion}} = 2\frac{D}{(L/2)^2} = 8\frac{\mu k_b T}{qL^2} \tag{4}$$

where k_b is the Boltzmann constant, T the temperature, and q the elementary charge.[10] Thus, according to Equation (3), when the applied voltage (V_a) cancels the built-in electric field, the effective voltage (V_{eff}) and so the drift rate are zero. In this condition, the extraction rate is minimum and only due to the diffusion rate, which does not depend on the applied voltage, see Equation (4). Therefore, the mobility can be easily calculated by measuring the minimum of the extraction rate.

In a first approximation, the decay in current (J_{decay}) can be considered as proportional to the decay of Δq. Thus, solving Equation (1) gives

$$J_{\text{decay}} \propto \exp(-ft) \tag{5}$$

The expression of the current decay, described above, shows that with a simple exponential fit of the current decay the extraction rate can be calculated. Hence, by finding the voltage where the extraction rate is minimum, the mobility value can be determined. The effect of the recombination is neglected in the expression of the current in Equation (5) because the recombination has a limited effect on the calculated mobility for reasonable mobilities and recombination rate constant values. In fact, as shown in Figure S1 (Supporting Information) for very typical value of the recombination rate constant, see the Supporting Information for more details, the calculated mobility only vary by a factor ≈2, which is also similar to the experimental error when using the SCLC technique. The change of any injection barriers also has a negligible effect on the calculated mobility as shown in Figure S2 (Supporting Information).

The advantage of this technique is that the device is maintained under conditions close to realistic operating conditions with an illumination intensity always close to 1 sun and under constant bias, as opposed to other transient techniques, such as

TOF,[5a] time-resolved electric-field-induced second harmonic generation (TREFISH)/TOF,[6b,c] and transient photocurrent (TPC),[11] which are based on pulsed light. Keeping the device under illumination and bias close to the maximum power point ensures that the charge carrier densities[12] and the electrical field,[12b] which can influence the charge carrier motion, will be similar to those observed in a working solar cell leading to a characterization of the transport properties closer to what happens under steady-state conditions.

Secondly, to validate the assumptions made above a transient 1D drift-diffusion simulation was set up. In this simulation, the active layer of the BHJ solar cell is modeled using an effective medium approximation that considers the BHJ as a one-phase semiconductor. The highest occupied molecular orbital (HOMO) of the effective semiconductor is taken as the HOMO value of the donor, and the lowest unoccupied molecular orbital (LUMO) of the effective semiconductor is taken as the LUMO value of the acceptor. The model describes the movement of the charges by drift due to the electric field and diffusion due to the gradient of charge carrier concentration, more details can be found in ref. [13]. The simulations also account for bimolecular recombination within the active layer, calculated using reduced Langevin law,[14] as it is commonly seen as the main recombination pathway limiting the performance of high-efficiency OPV devices.[15] One should also note that the drift-diffusion equations use the steady-state mobilities as an input and do not include any effects of charge carrier dispersion. So the dispersion in photocurrent observed in other reports[6b,c] cannot be reproduced by the drift-diffusion simulation. However, these simulations are suitable in our case as this study aims to show that steady-state mobilities are the relevant parameters for OPV devices. In addition, if the drift-diffusion simulation can reproduce the experimental data, then dispersion does not play a significant role.

The simulation was first performed considering balanced mobilities. As shown in Figure 1, the exponential fit accurately reproduces the current decay. The fitting is performed for different applied voltage and the extraction rate is calculated using Equation (5), see **Figure 2**a. The clear dependence of the extraction rate on applied voltage, as expected from Equations (2)–(4), is in fact observed. A minimum in extraction rate can be noticed when the extraction is only due to diffusion, $f = f^{\text{Diffusion}}$, at this point Equation (4) can be used to calculate the value of the mobility. In the case of $\mu_n = \mu_p = 1 \times 10^{-7}$ m^2 V^{-1} s^{-1}, the calculated mobility is equal to 1.2×10^{-7} m^2 V^{-1} s^{-1}, thus the values obtained by the fit give values close to the input steady-state mobilities.

The same simulation was done for several ratios of the mobilities, and as the ratio increases the effect of the drift becomes less dominant and diffusion starts to play a more important role, Figure 2b. This observation is in agreement with the space charge effect observed in OPV devices with unbalanced mobilities, as the space charge creates an electrical field that shields the built-in field.[4c,7a] As in classic TPC, it is not possible with this experiment to dissociate the effect of the two carrier species.[11] However, as shown in **Table 1**, the mobilities calculated using Equation (4) are close to the geometrical average of the electron and hole mobilities. To conclude these simulations show that the simple model proposed previously is valid when there is no dispersion and that the mobility can be calculated using this simple experiment. In the following, the geometrical average of the steady-state mobilities will be used as a reference.

Finally, to validate the hypothesis that the steady-state mobilities govern the extraction in OPV devices, the experiment presented previously was conducted for several donor:acceptor blends. If the mobilities obtained by the experiment are the same as the one obtained with the SCLC technique, it would mean that the steady-state mobilities are in fact relevant to characterize the extraction and transport in the case of OPV devices. Solar cells, made of polythieno[3,4-*b*]-thiophene-*co*-benzodithiophene (PTB7) mixed with [6,6]-phenyl-C71-butyric acid methyl ester (PC[70]BM), successfully illustrate the behavior presented previously, see **Figure 3**. In fact, a clear minimum of the extraction rate at $V_a = 0.7$ V and a well-defined effect of the drift are observed, as expected from Equation (3). The decay

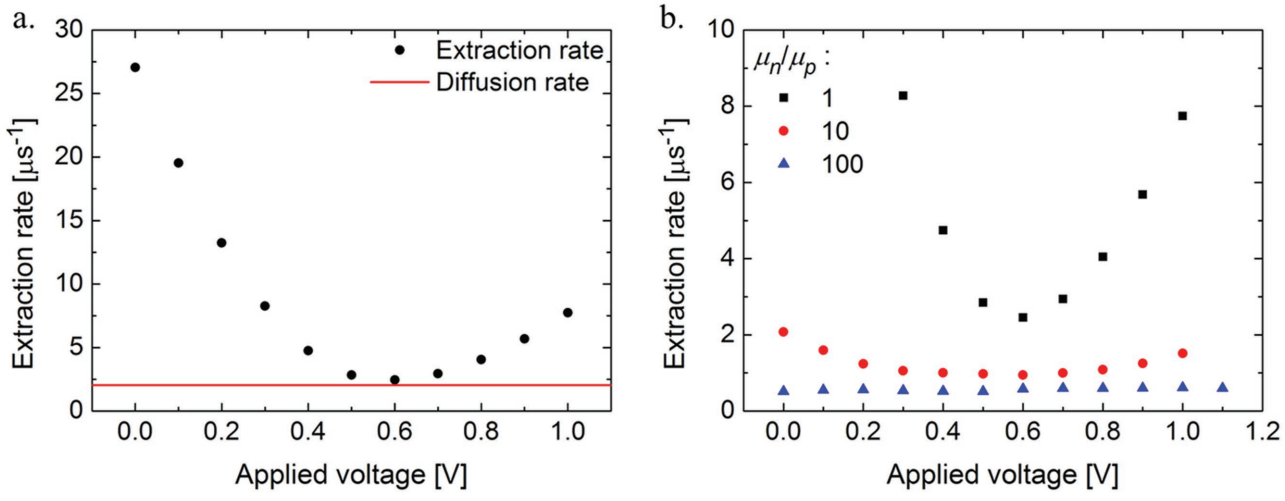

Figure 2. a) Extraction rate for balanced mobilities, $\mu_n = \mu_p = 1 \times 10^{-7}$ m^2 V^{-1} s^{-1}, symbols, and minimum diffusion rate, red line, calculated with Equation (4). b) Extraction rate for different mobility ratios.

Table 1. Extraction rate for different mobility ratios.

μ_n [$m^2 V^{-1} s^{-1}$]	μ_p [$m^2 V^{-1} s^{-1}$]	Ratio	Average $\mu^{a)}$ [$m^2 V^{-1} s^{-1}$]	Extracted $\mu^{b)}$ [$m^2 V^{-1} s^{-1}$]
1×10^{-7}	1×10^{-7}	1	1×10^{-7}	1.2×10^{-7}
1×10^{-7}	1×10^{-8}	10	3.2×10^{-8}	4.7×10^{-8}
1×10^{-7}	1×10^{-9}	100	1×10^{-8}	2.6×10^{-8}

[a)]Geometrical average: $\mu = \sqrt{\mu_n \mu_p}$; [b)]Using Equation (4).

of the current (see Figure 3b) also fits well with the model described above, showing an exponential decay. The measured mobility, $\mu = 4 \times 10^{-8}$ m^2 V^{-1} s^{-1}, is coherent with the geometrical average of the mobilities obtained from the SCLC measurement, $\mu = 3.2 \times 10^{-8}$ m^2 V^{-1} s^{-1}.[7b]

As the aim of this study is to show that these results can be broadened to other organic materials this experiment has been conducted on other blends. PC[70]BM and PC[60]BM have been used as acceptor blended with different donor polymers: MEH-PPV, P3HT, PTB7, PDPP5T, PBDTT-FTTE, PBDTTT-C, see full names in the Experimental Section. These polymers have been chosen so that the resulting blends cover a wide range of mobility values from 10^{-9} to 10^{-7} m^2 V^{-1} s^{-1}, mobility ratio from 1 to 100, and efficiency from 2 to 3% in the case of P3HT:PC[60]BM to 8–9% for PBDTT-FTTE:PC[70]BM cell, see **Table 2** and Figure S4 (Supporting Information). The tested blends give similar results as shown previously for PTB7:PC[70]BM blends. The extracted mobility is in fact always close to the geometrical average of the measured SCLC mobilities, see Table 2 and Figure S4 (Supporting Information). One can also note that the obtained values are the same if a larger reduction of the light intensity is performed. In fact, even when studying the most extreme case, which is light to dark transition, the lifetime obtained are the same, see Figure S4 (Supporting Information). It also means that the extracted mobility reflects the behavior of all the charge carriers.

In addition, the integration of the current decay makes it possible to measure the half-life time that shows that ≈1 µs is needed to extract 50% of the carriers; see Table 2. The microsecond time scale is far from the nanosecond time scale that has been reported by other groups in the case of extraction dominated by dispersion.[6b,c] These two findings confirm that charge carrier thermalization has a limited effect on the device extraction when the devices are tested under realistic operating conditions. It is also in agreement with the conclusion of van der Kaap and Koster on organic diodes, where they have demonstrated that the steady-state mobility is only slightly enhanced, when the relaxation of high energetic charge carriers is taken into account, compared to the value in thermal equilibrium.[6a]

One could ask why the results obtained here differ from the conclusion obtained in other papers and why here the thermal relaxation of the "hot" carriers appears to make a limited contribution to the extraction. It can be explained by the fact that the testing conditions greatly influence the results and that care should be taken when choosing the conditions under which the transport will be characterized. For example the temperature, the fact to be under constant illumination and the background charge carrier densities have an influence on the relative importance of the "hot" carrier relaxation.[5,6] In preceding experiments and simulations,[6b,c] the characterization of the transport is based on pulsed light on a device otherwise in the dark, that is, in the situation where the DOS is empty, see **Figure 4**a. Thus, the charge carriers generated by the light pulse never have the chance to reach a steady-state-like condition as they can go through the DOS without reaching a point where they will have to move through hoping close to the equilibrium level, see Figure 4b(2).[16] This can explain the high charge carrier mobilities and strong dispersion effect observed by these reports. However, as shown in Figure 4b, when the device is under steady-state condition the bottom of the DOS is filled hence the relaxation time of the charge carrier is much faster, as shown by van der Kaap and Koster in ref. [6a]. After they relax the charge carriers have to move by hopping around the

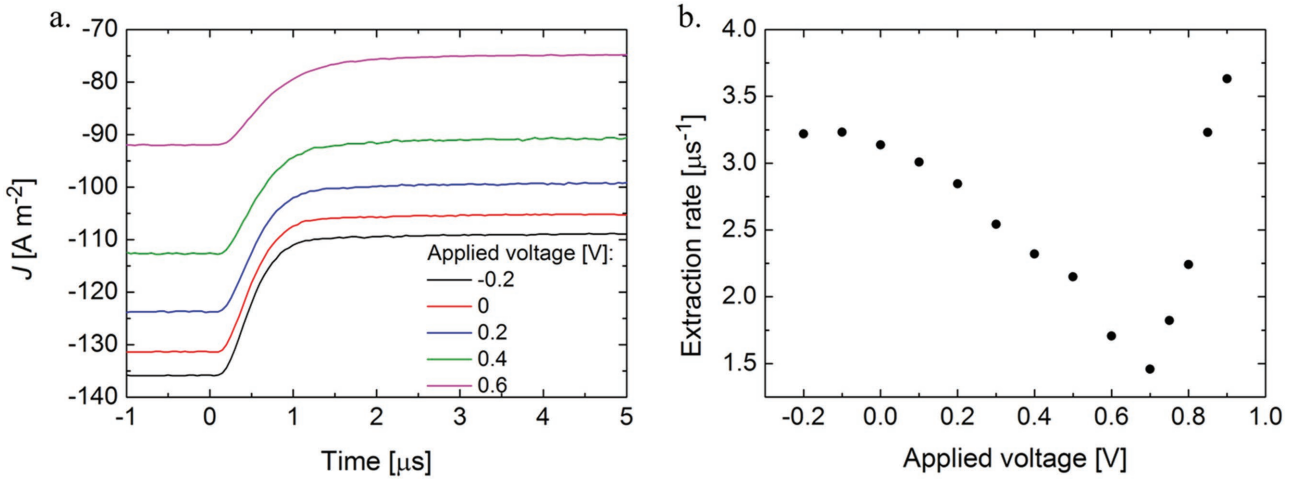

Figure 3. Experimental results for a PTB7:PC[70]BM solar cell showing a) the extracted current for different applied voltage and b) the extraction rate, calculated with Equation (5). These two results show the same trend that the results obtained with the drift-diffusion simulation in Figures 1 and 2.

Table 2. Extraction rate for different acceptor:donor blends.

Blend	μ_n [$m^2 V^{-1} s^{-1}$]	μ_p [$m^2 V^{-1} s^{-1}$]	Average $\mu^{a)}$ [$m^2 V^{-1} s^{-1}$]	Extracted $\mu^{b)}$ [$m^2 V^{-1} s^{-1}$]	Half-life time [μs]
MEH-PPV:PC[60]BM	1×10^{-9} [c)]	2.5×10^{-9} [c)]	1.6×10^{-9}	1.9×10^{-9}	2.8
P3HT:PC[60]BM	1.9×10^{-7} [10]	3.7×10^{-9} [10]	2.7×10^{-8}	3.4×10^{-8}	1.0
PTB7:PC[70]BM	3.5×10^{-8} [7b]	3×10^{-8} [7b]	3.2×10^{-8}	4.0×10^{-8}	0.48
PDPP5T:PC[70]BM	3.1×10^{-7} [7b]	2.9×10^{-7} [7b]	3.0×10^{-7}	1.3×10^{-7}	0.58
PBDTT-FTTE:PC[70]BM	1.3×10^{-7} [c)]	3.3×10^{-8} [c)]	6.5×10^{-8}	8.8×10^{-8}	0.45
PBDTTT-C:PC[70]BM	2.1×10^{-8} [c)]	8×10^{-9} [c)]	1.3×10^{-8}	6.0×10^{-8}	0.97

[a)]Geometrical average: $\mu = \sqrt{\mu_n \mu_p}$; [b)]Using Equation (4); [c)]Figure S5 (Supporting Information).

equilibrium level[16] leading to the mobility commonly observed in steady-state measurement. The case described in Figure 4b is more likely to describe what we observed in our experiment. One should note that the drawing depicted in Figure 4 is not intended to represent a specific shape of the DOS. In a disordered system, the DOS will be smeared out (e.g., exponential, Gaussian) which will induce some form of dispersion as hot carriers can relax in the DOS. In both the exponential DOS and the Gaussian case, the mobility depends on the filling of the DOS.[12] However, the typical density of carriers in a solar cell under illumination is low (as compared to field-effect transistors, for example) typically between 10^{21} and 10^{22} m^{-3},[13a] which means that the effect of illumination on mobility is not strong. However, charges that are photogenerated high up in the DOS will still thermalize and cause dispersion. In the present paper, we show that this thermalization is so rapid that it does not affect the extraction from an organic solar cell. To summarize, if one wants to make any statements on the transport and extraction in OPV devices, one must take care to choose operating conditions such that they reflect the real states of a working solar cell. Moreover, Blakesley and Neher have shown that a high amount of disorder is detrimental to the open-circuit voltage and would limit the efficiency.[17] So designing highly disordered materials that would benefit from the effect of the dispersion is not the best road to achieve high efficiency as it would lead to devices with a low open-circuit voltage.

3. Conclusion

In conclusion, we have shown that the dispersion of the current plays a limited role in the charge carrier extraction in OPV devices. This result is supported by experimental data, for several donor:acceptor blends, which constantly show mobilities and half-life time on the same order of magnitude as those expected for the mobilities measured using the classic SCLC technique. In addition, the good agreement between drift-diffusion simulation and experimental results also shows that steady-state mobilities are sufficient to characterize the transport and extraction in OPV devices. Thus, steady-state mobilities that are found by SCLC technique give a valuable insight into the performance of OPV materials.

4. Experimental Section

The solar cells were fabricated using polythieno[3,4-*b*]-thiophene-co-benzodithiophene (PTB7) (purchased from Solarmer), poly(3-hexylthiophen-2,5-diyl) (P3HT) (purchased from Rieke Metals Inc),

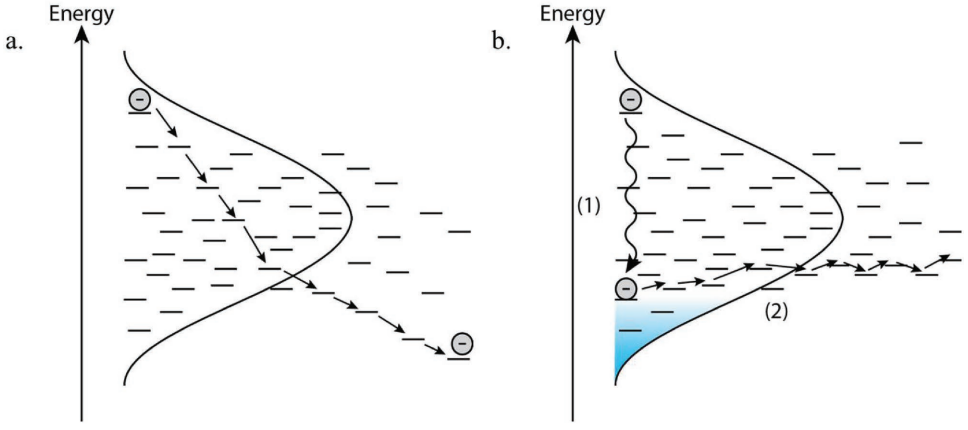

Figure 4. Different dynamics of charge carrier extraction depending on the illumination: a) fast extraction of high energetic carriers generated in an empty DOS, that is, by a pulse of light in the dark; b) fast relaxation of the charge carrier (1) followed by a transport by hopping when reaching the bottom of the DOS which is filled due to the constant illumination (2).

a small bandgap diketopyrrolopyrrole-quinquethiophene alternating copolymer (PDPP5T),[18] poly[2-methoxy-5-(2-ethylhexyloxy)-1,4-phenylenevinylene] (MEH-PPV), PBDTT-FTTE (purchased from Solarmer) and PBDTTT-C (purchased from Solarmer) as donor, and [6,6]-phenyl-C61-butyric acid methyl ester (PC[60]BM) or [6,6]-phenyl-C71-butyric acid methyl ester (PC[70]BM) (purchased from Solenne) as acceptor.

Structured indium tin oxide (ITO) was used as substrate. All substrates were cleaned with soap water for 5 min, followed by deionized water flushing, and subsequently 10 min ultrasonic bath in acetone and isopropyl alcohol. Finally, the substrates were spin-dried and transferred into the oven for 10 min, followed by UV–ozone treatment for 20 min. A 50 nm poly(3,4-ethylenedioxythiophene):poly (styrene sulfonate) (PEDOT:PSS) was then spin-cast on the substrate, followed by 10 min oven drying to remove the residual water.

PTB7:[60]PCBM Solar Cells: A solution of PTB7:PC[70]BM (1:1.5 by weight) in 1,2-dichlorobenzene from PTB7 (16 mg mL^{-1}) and PC[70]BM (24 mg mL^{-1}) was spin-coated at 600 rpm for 120 s, yielding an active layer of around 80 nm.

P3HT:PC[60]BM Solar Cells: A solution of P3HT:PC[60]BM blend (1:1 by weight) in chloroform with a concentration of either 10 mg mL^{-1} was spin-coated at 300 rpm for 50 s, yielding active layers of around 100 nm thick. The active layer was then annealed at 140 °C for 5 min.

PDPP5T:PC[70]BM Solar Cells: The blend (1:2 by weight with a total concentration of 20 mg mL^{-1}) was spin-cast from chloroform/*ortho*-dichlorobenzene (5% vol) solution in N_2 atmosphere. Spin-coating with 1000 rpm for 120 s yielded an active layer of 150 nm thick. The active layer was finally left to dry at room temperature before depositing the cathode.

MEH-PPV:PC[60]BM Solar Cells: A solution of MEH-PPV:PC[60]BM blend (70%wt MEH-PPV) in chlorobenzene with a total concentration of 10 mg mL^{-1} was spin-coated at 1000 rpm for 120 s, yielding an active layer of around 40 nm thick.

PBDTT-FTTE and PBDTTT-C Solar Cells: The solutions were fabricated with a mixture of individual polymers with PC[70]BM dissolved in *ortho*-dichlorobenzene in a ratio of 1:1.5 of polymer:fullerene with a 10 mg mL^{-1} of the polymer concentration. The solutions were stirred overnight on a hot plate kept at 60 °C. Prior to their spin-casting on ITO/PEDOT:PSS at 800 rpm for 5 s with lid closed and spin-dried at 400 rpm for 180 s with lid opened in N_2-filled glovebox the solutions were removed from the hot plate but kept stirred for at least 30 min.

After depositing the active layer all the cells were finished by thermally evaporated LiF (1 nm) and Al (100 nm) through shadow masks in a vacuum chamber at 10^{-6} mbar, defining an active area of 1 mm^2.

Hole and electron-only devices were made with the following device structure: glass/Cr (1 nm)/Au (20 nm)/PEDOT:PSS/active layer/Pd (15 nm)/Au (80 nm) and glass/Al (20 nm)/active layer/LiF (1 nm)/Al (100 nm), respectively.

Electrical measurements of the current–voltage characteristics of all the devices were performed using a computer-controlled Keithley source meter in N_2 atmosphere. The measurements under illumination were done using a Steuernagel SolarConstant 1200 metal halide lamp; a silicon reference cell was employed to correct for the spectral mismatch with AM1.5G spectrum and set the intensity of the lamp to 1 sun.

Transient measurements were performed using a biased white light LED with an on/off switch time of ≈100 ns. The corresponding transient signals were recorded using a digital storage oscilloscope DSO-X 3034A.

Supporting Information

Supporting Information is available from the Wiley Online Library or from the author.

Acknowledgements

This work was supported by a grant from STW/NWO (VIDI 13476). This is a publication by the FOM Focus Group "Next Generation Organic Photovoltaics," participating in the Dutch Institute for Fundamental Energy Research (DIFFER).

Conflict of Interest

The authors declare no conflict of interest.

Keywords

bulk-heterojunction solar cells, charge carrier extraction, organic photovoltaics, steady-state mobility

Received: April 25, 2017
Revised: June 9, 2017
Published online: September 11, 2017

[1] N. S. Sariciftci, D. Braun, C. Zhang, V. I. Srdanov, A. J. Heeger, G. Stucky, F. Wudl, *Appl. Phys. Lett.* **1993**, *62*, 585.

[2] a) J. Zhao, Y. Li, G. Yang, K. Jiang, H. Lin, H. Ade, W. Ma, H. Yan, *Nat. Energy* **2016**, *1*, 15027; b) Heliatek, Organic Photovoltaic World Record Efficiency of 13.2%, **2016**; c) NREL, *Best Research-Cell Efficiencies*, http://www.nrel.gov/ncpv/images/efficiency_chart.jpg (accessed: August 2016).

[3] a) J. L. Bredas, J. P. Calbert, D. A. da Silva Filho, J. Cornil, *Proc. Natl. Acad. Sci. USA* **2002**, *99*, 5804; b) V. Coropceanu, J. Cornil, D. A. da Silva Filho, Y. Olivier, R. Silbey, J.-L. Brédas, *Chem. Rev.* **2007**, *107*, 926.

[4] a) J. C. Blakesley, F. A. Castro, W. Kylberg, G. F. A. Dibb, C. Arantes, R. Valaski, M. Cremona, J. S. Kim, J.-S. Kim, *Org. Electron.* **2014**, *15*, 1263; b) V. D. Mihailetchi, H. X. Xie, B. de Boer, L. J. A. Koster, P. W. M. Blom, *Adv. Funct. Mater.* **2006**, *16*, 699; c) V. D. Mihailetchi, J. Wildeman, P. W. M. Blom, *Phys. Rev. Lett.* **2005**, *94*, 126602.

[5] a) L. Pautmeier, R. Richert, H. Bässler, *Synth. Met.* **1990**, *37*, 271; b) P. M. Borsenberger, E. H. Magin, M. D. Van Auweraer, F. C. De Schryver, *Phys. Status Solidi A* **1993**, *140*, 9.

[6] a) N. J. van der Kaap, L. J. A. Koster, *Sci. Rep.* **2016**, *6*, 19794; b) A. Melianas, V. Pranculis, A. Devižis, V. Gulbinas, O. Inganäs, M. Kemerink, *Adv. Funct. Mater.* **2014**, *24*, 4507; c) A. Melianas, F. Etzold, T. J. Savenije, F. Laquai, O. Inganas, M. Kemerink, *Nat. Commun.* **2015**, *6*, 8778.

[7] a) J. A. Bartelt, D. Lam, T. M. Burke, S. M. Sweetnam, M. D. McGehee, *Adv. Energy Mater.* **2015**, *5*, 1500577; b) D. Bartesaghi, I. d. C. Perez, J. Kniepert, S. Roland, M. Turbiez, D. Neher, L. J. A. Koster, *Nat. Commun.* **2015**, *6*, 7083; c) C. M. Proctor, J. A. Love, T.-Q. Nguyen, *Adv. Mater.* **2014**, *26*, 5957; d) D. Neher, J. Kniepert, A. Elimelech, L. J. A. Koster, *Sci. Rep.* **2016**, *6*, 24861.

[8] a) D. Rezzonico, B. Perucco, E. Knapp, R. Häusermann, N. A. Reinke, F. Müller, B. Ruhstaller, *J. Photonics Energy* **2011**, *1*, 011005; b) J. J. Brondijk, F. Torricelli, E. C. P. Smits, P. W. M. Blom, D. M. de Leeuw, *Org. Electron.* **2012**, *13*, 1526; c) R. Häusermann, E. Knapp, M. Moos, N. A. Reinke, T. Flatz, B. Ruhstaller, *J. Appl. Phys.* **2009**, *106*, 104507.

[9] S. Albrecht, W. Schindler, J. Kurpiers, J. Kniepert, J. C. Blakesley, I. Dumsch, S. Allard, K. Fostiropoulos, U. Scherf, D. Neher, *J. Phys. Chem. Lett.* **2012**, *3*, 640.

[10] L. J. A. Koster, M. Kemerink, M. M. Wienk, K. Maturová, R. A. J. Janssen, *Adv. Mater.* **2011**, *23*, 1670.

[11] J. Seifter, Y. Sun, A. J. Heeger, *Adv. Mater.* **2014**, *26*, 2486.

[12] a) C. Tanase, E. J. Meijer, P. W. M. Blom, D. M. de Leeuw, *Phys. Rev. Lett.* **2003**, *91*, 216601; b) W. F. Pasveer, J. Cottaar, C. Tanase,

R. Coehoorn, P. A. Bobbert, P. W. M. Blom, D. M. de Leeuw, M. A. J. Michels, *Phys. Rev. Lett.* **2005**, *94*, 206601.
[13] a) L. J. A. Koster, E. C. P. Smits, V. D. Mihailetchi, P. W. M. Blom, *Phys. Rev. B* **2005**, *72*, 085205; b) S. Selberherr, *Analysis and Simulation of Semiconductor Devices*, Springer-Verlag, Wien, Germany, **1984**, p. 285.
[14] P. Langevin, *Ann. Chim. Phys.* **1903**, *28*, 433.
[15] a) A. R. G. Lakhwani, R. H. Friend, *Annu. Rev. Phys. Chem.* **2014**, *65*, 557; b) A. Foertig, J. Kniepert, M. Gluecker, T. Brenner, V. Dyakonov, D. Neher, C. Deibel, *Adv. Funct. Mater.* **2014**, *24*, 1306; c) J. Kniepert, I. Lange, N. J. van der Kaap, L. J. A. Koster, D. Neher, *Adv. Energy Mater.* **2014**, *4*, 1301401.
[16] J. J. M. van der Holst, F. W. A. van Oost, R. Coehoorn, P. A. Bobbert, *Phys. Rev. B* **2011**, *83*, 085206.
[17] J. C. Blakesley, D. Neher, *Phys. Rev. B* **2011**, *84*, 075210.
[18] V. S. Gevaerts, A. Furlan, M. M. Wienk, M. Turbiez, R. A. J. Janssen, *Adv. Mater.* **2012**, *24*, 2130.